

Proceeding Paper

# Research on Asymmetrical Reinforced Concrete Low-Rise Frames under Multiple Seismic Events <sup>†</sup>

Paraskevi K. Askouni 

Department of Civil Engineering, University of Patras, 26504 Patras, Greece; askounie@upatras.gr

<sup>†</sup> Presented at the 1st International Online Conference on Buildings, 24–26 October 2023; Available online: <https://iocbd2023.sciforum.net/>.

**Abstract:** Current seismic regulations neglect the influence of multiple seismic events on the seismic response, which, as already recognized in the literature, may influence the seismic behavior of reinforced concrete structures. Symmetrical and asymmetrical low-rise reinforced concrete frames are investigated here via nonlinear time-history (NLTH) analysis considering multiple earthquake events, as well as under a respective single seismic event, for comparison purposes. The two horizontal directions, as well as the vertical one, of the ground excitation are considered in the dynamic analysis, assuming the elastoplastic action of reinforced concrete sections under heavy loading. A simple ratio is defined to express the geometrical in-plane asymmetry of the buildings. The nonlinear response outcomes of the time-history analyses are appropriately plotted by using unitless parameters for an objective estimation of the structural behavior under multiple earthquakes. The dimensionless response results and plots are presented and discussed in view of the relative geometrical asymmetry of the 3D frames. The effect of the multiple seismic events, as well as the one of a simple geometrical symmetry/asymmetry, is identified and discussed in the presented plots resulting from the dynamic analysis. Thus, practical remarks are presented regarding the significance of the in-plane symmetry/asymmetry of frames for improvements in the provisions of the current seismic regulations to develop safer structures.

**Keywords:** multiple seismic events; earthquake; symmetry; asymmetry; reinforced concrete; time-history analysis; nonlinear behaviour



**Citation:** Askouni, P.K. Research on Asymmetrical Reinforced Concrete Low-Rise Frames under Multiple Seismic Events. *Eng. Proc.* **2023**, *53*, 29. <https://doi.org/10.3390/IOCBD2023-15191>

Academic Editor: Humberto Varum

Published: 24 October 2023



**Copyright:** © 2023 by the author. Licensee MDPI, Basel, Switzerland. This article is an open access article distributed under the terms and conditions of the Creative Commons Attribution (CC BY) license (<https://creativecommons.org/licenses/by/4.0/>).

## 1. Introduction

Geometrical structural asymmetry is mentioned in existing research to influence the seismic response, e.g., in Rutenberg [1], Goel and Chopra [2] and Bento et al. [3], in addition to plenty of research that has already been performed on reinforced concrete common buildings, dimensioned to current regulations, such as Eurocode 2 (EC2) [4] following the seismic guidelines of Eurocode 8 (EC8) [5]. However, the current seismic design codes, e.g., EC8 [5], tend to ignore the role of multiple seismic events on the structural response, though identified by other research works, such as refs. [6–8]. The current paper aims to point out the significance of multiple ground excitation events on the behavior of common, symmetric/asymmetric low-rise 3D frames.

## 2. Description of Frames and Analysis

Common low-rise 3D reinforced concrete (RC) framed buildings, as shown in Figure 1, are subject to multiple earthquakes. The investigated one- and three-story frames have in-plane dimensions of  $5.0 \times 4.0 \text{ m}^2$ . The first story has a height of 4.0 m, while the second and third ones possess a height of 3.0 m each. The RC beams have sectional dimensions of  $0.25 \times 0.60 \text{ m}^2$ . The three RC columns have the same dimensions,  $0.40 \times 0.40 \text{ m}^2$  for the first story and  $0.35 \times 0.35 \text{ m}^2$  for higher ones, while the fourth column has an in-steps-variable cross-section from the previous values up to  $0.30 \times 2.0 \text{ m}^2$ , called “wall” here.

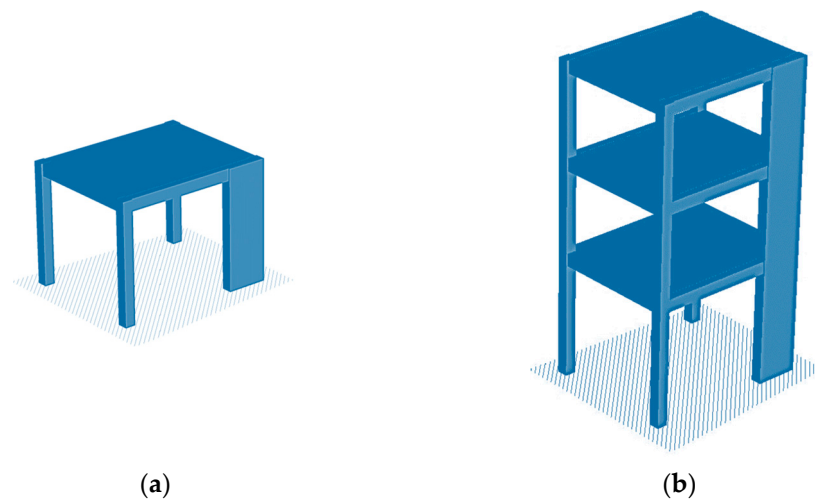


**Figure 1.** Asymmetrical RC buildings with (a) one story and (b) three stories.

The examined buildings are constructed using concrete C20/25 reinforced with steel B500c, designed and detailed following the current codes, EC2 [4] and EC8 [5], where the considered loadings follow Eurocode 1 [9], and their combinations are according to [5], considering the characteristic 30% provision [5] and the “accidental eccentricity” of 5% [5]. The dimensioning and design assumptions consider typical domestic buildings for a ductility class medium (DCM) [4,5], zone ground acceleration 0.36 g, 5% viscous damping ratio, soil type C and the usual rigid soil assumption. The behavior factor [5] of each frame is estimated separately according to current codes. The capacity design rules of EC2 [4] and EC8 [5] are considered in the detailing of main structural elements and their connections against “shear” [5].

The “non-linear time-history (NLTH) analyses” [10] are accomplished using the software ETABS [11] for the following multiple 3D seismic events, as downloaded from [12]: “Chalfant Valley” [12], in 1986, characterized by two events; the “Coalinga” [12], in 1983, by two events; “Imperial Valley” [12], in 1979, by two events; “Mammoth Lakes” [12], in 1980, by five events; and “Whittier Narrows” [12], in 1987, by two events. Similarly, to [6,7,10], for each ground motion, between the seismic events, a time-frame of 100s with acceleration values equal to zero is considered to reduce the structural vibration caused by damping. In addition, the frames are analyzed under the first excitation of the “Mammoth Lakes” excitation, referred to here as “Mammoth-1st”, to compare the effect of one event to multiple ones. The angle of the earthquake direction is chosen as “ $\theta = 0^\circ$ ,  $\theta = 90^\circ$  and  $\theta = 45^\circ$ ” [10], corresponding to the basic horizontal and diagonal axes, to inquire about this impact on the dynamic response, as identified by previous works [10,13]. The nonlinear attitude of RC sections is regarded through the application of elastoplastic hinges at structural linear element ends at the analysis model of ETABS [11], where the main nonlinear features, e.g., reduced stiffness, limit bending moments, etc., are calculated following refs. [4,5,14,15].

### 3. Seismic Response Results

The arithmetical outcomes of the NLTH analyses of the frames under the multiple seismic events are presented and discussed. The asymmetry of the frames is induced by the asymmetry of the wall element compared to the column, where a division of the later sections provides a simple dimensionless ratio, mentioned here as “A(wall)/(col)”, appropriate for the study of the analysis outcomes. Due to limited space, selected charts are shown regarding the “interstory drift ratio” (“IDR”) [10,16] and the “residual IDR” (“RIDR”) [10] comparatively to the constraints of the “performance levels” [16] for reinforced concrete buildings. For reading convenience, the limits of IDR are mentioned as 0.01, corresponding to the “Immediate Occupancy (IO)” “performance level” [16], 0.02 to the “Life Safety (LS) performance level” [16] and 0.04 to the “Collapse Prevention (CP)

performance level” [16]. Respectively, the RIDR limits are mentioned as negligible for the IO stage [16], 0.01 for the LS stage [16] and 0.04 for the CP stage [16]. For purposes of brevity, each earthquake is mentioned by its name followed by (0), (45) or (90) for each angle of the ground excitation of 0°, 45° or 90°, respectively.

### 3.1. One-Story Frames

For one-story frames, the IDR-X for  $\theta = 45^\circ$  in Figure 2a tends to slightly decrease as the wall section becomes greater within the LS stage limit [16]. The IDR-Y for  $\theta = 0^\circ$  variably decreases as the wall section increases (Figure 2b), with higher average values than the IDR-X plot (Figure 2a). In Figure 2a,b, the gap of IDR plots at both axes for the symmetrical case mentions IDR values much higher than all limits of [16], meaning a strength lack of the symmetric frame for the multiple seismic events of Chalfant Valley.

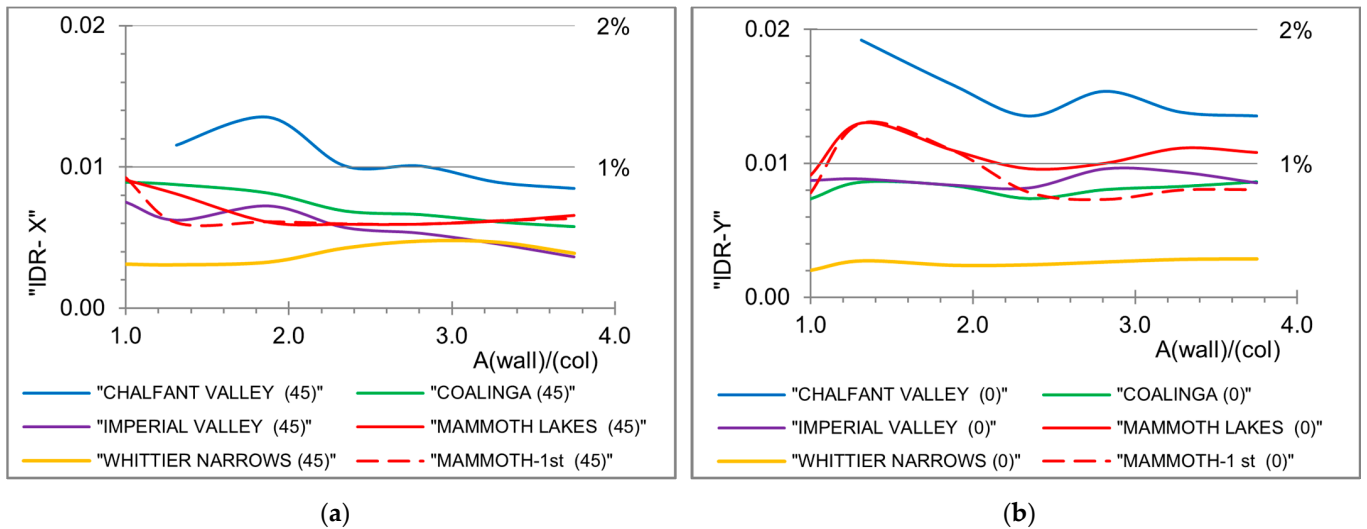


Figure 2. (a) Interstory drift ratio on X,  $\theta = 45^\circ$ , (b) interstory drift ratio on Y,  $\theta = 0^\circ$ .

The RIDR chart shows fluctuating plotlines (Figure 3), with a range of values within 0~0.0024 at the X axis,  $\theta = 90^\circ$  and 0~0.003 at the Y axis,  $\theta = 90^\circ$ , within the LS stage [16]. The discontinuity of the RIDR plotlines for the “Chalfant Valley” excitation indicates the building deficiency in the symmetric frame for this sequential earthquake.

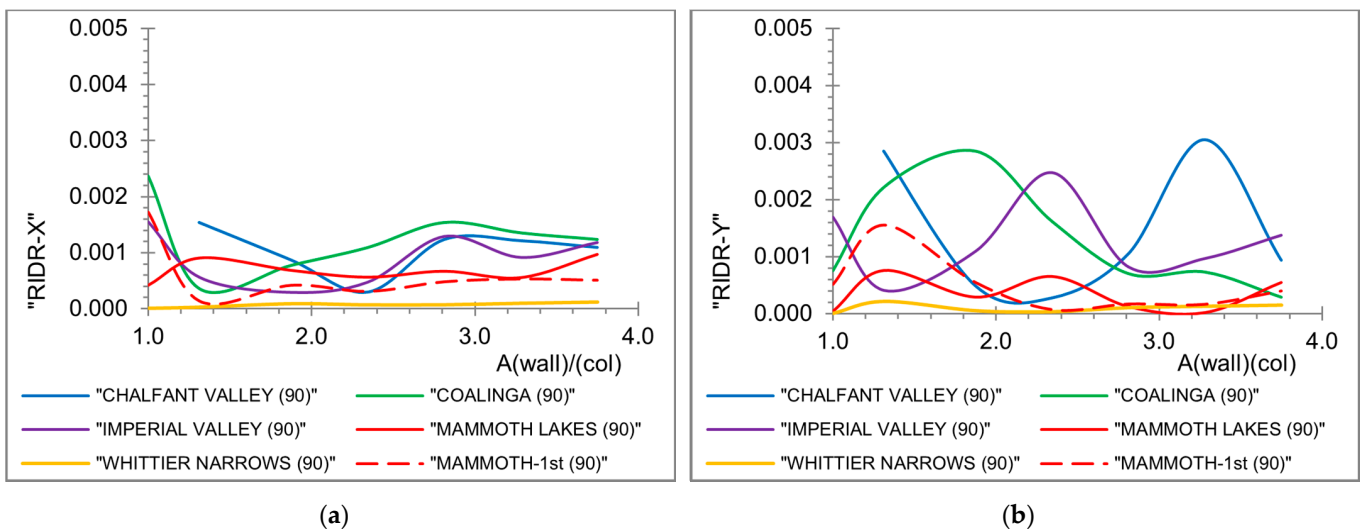


Figure 3. (a) Residual interstory drift ratio on X,  $\theta = 90^\circ$ , (b) residual interstory drift ratio on Y,  $\theta = 90^\circ$ .

### 3.2. Three-Story Frames

For the three-story frames, concerning the first story, the IDR on the X axis,  $\theta = 0^\circ$ , drops as the wall section increases inside the restriction of 0.02 for the LS stage [16] (Figure 4a). The IDR on the Y axis,  $\theta = 90^\circ$ , (Figure 4b) fluctuates as the wall section increases inside the limit of 0.02 similar to the previous chart (Figure 4a).

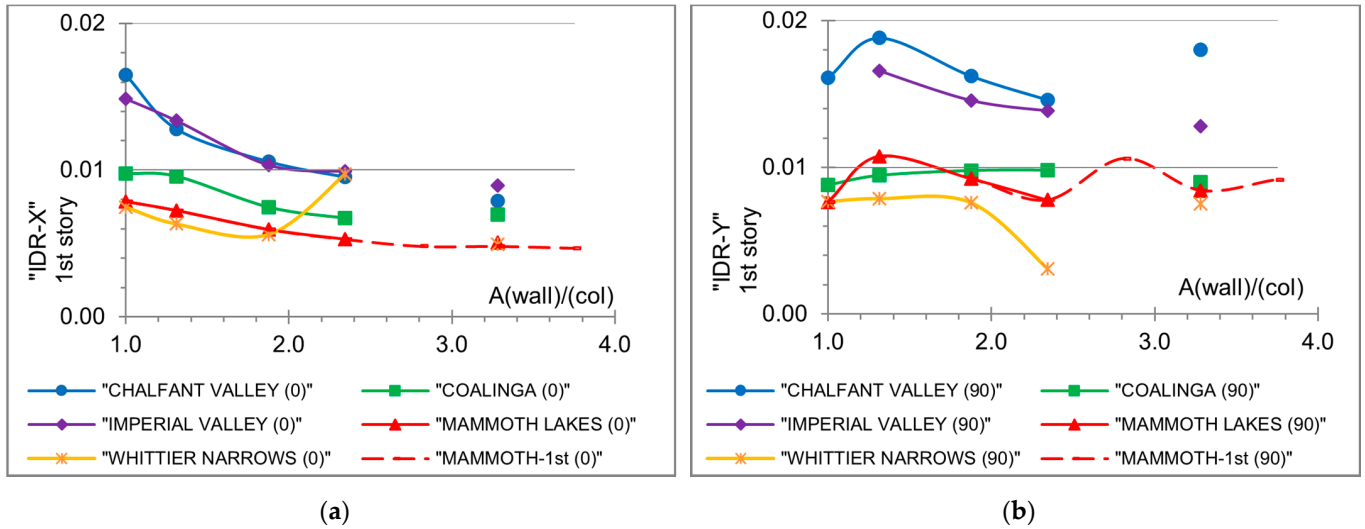


Figure 4. (a) Interstory drift ratio on X axis,  $\theta = 0^\circ$ , (b) interstory drift ratio on Y axis,  $\theta = 90^\circ$ , 1st story.

For the second story (Figure 5), both IDR on X for  $\theta = 0^\circ$  and IDR on Y for  $\theta = 90^\circ$  vary within 0.006~0.016, inside the LS performance level [16]. For the third story (Figure 6a), the IDR on the X axis,  $\theta = 90^\circ$ , even increases up to 0.024, which is over LS but within the CP level for the Chalfant Valley multiple events and has a value range within the LS level for the rest of the excitations. For the third story, the IDR-Y,  $\theta = 90^\circ$  (Figure 6b), shows an increasing tendency for all excitations, with values up to 0.019, within the LS performance level [16].

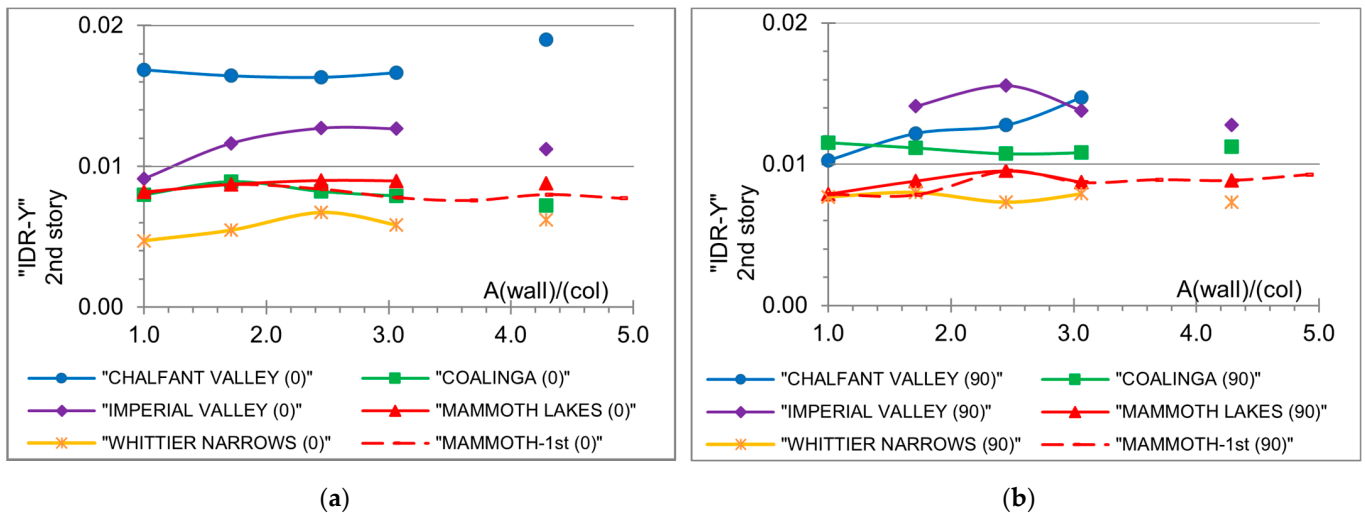


Figure 5. (a) Interstory drift ratio on X axis,  $\theta = 0^\circ$ , (b) interstory drift ratio on Y axis,  $\theta = 90^\circ$ , 2nd story.

For all stories, the gaps of the plotlines for the multiple seismic events represent the failure of the frames due to great exceedance of the IDR limits [16], as observed for the symmetric frame and wall sections of  $150 \times 30 \text{ cm}^2$  and  $200 \times 30 \text{ cm}^2$  in Figures 4a,b, 5a,b and 6a,b. However, for the single seismic event of Mammoth-1st, no failures are observed in Fig-

ures 4–6, which means an underestimation of the seismic response due to neglect of the sequential excitation.

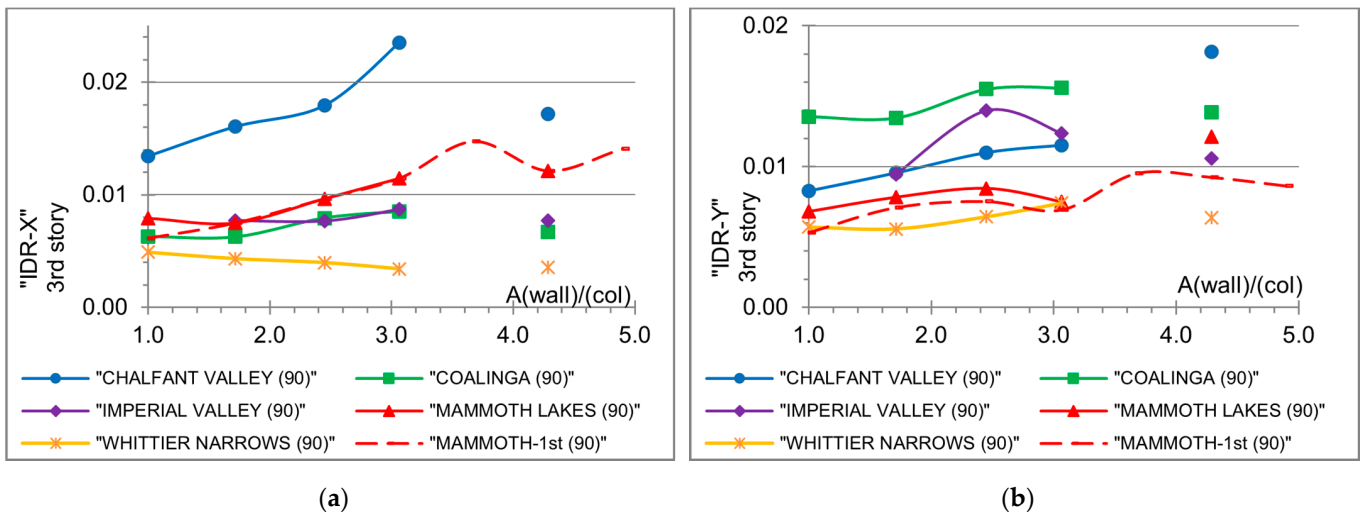


Figure 6. (a) Interstory drift ratio on X axis,  $\theta = 90^\circ$ , (b) interstory drift ratio on Y axis,  $\theta = 90^\circ$ , 3rd story.

As shown in Figure 7a, for the first story, the RIDR-X, for  $\theta = 45^\circ$ , varies within 0~0.002, i.e., lower than the limit in the LS stage [16]. Respectively, the RIDR-Y, for  $\theta = 45^\circ$ , is observed (Figure 7b) to vary in a range of 0~0.0028, inside the LS stage [16]. For the third story (Figure 8), the RIDR shows a variable value range of 0~0.0025 at the X axis for  $\theta = 45^\circ$  and 0~0.00376 at the Y axis for  $\theta = 0^\circ$ , where these ranges are smaller than the limit of the LS level [16]. The RIDR values are observed as greater at the Y axis than the ones at the X axis, in Figures 7 and 8. Similar to Figures 4–6, the discontinuities of the RIDR plot lines for great wall sections identify extreme RIDR values much higher than the limits of the current code [16], which means building failure for the repeated ground excitations, in contrast to the single excitation.

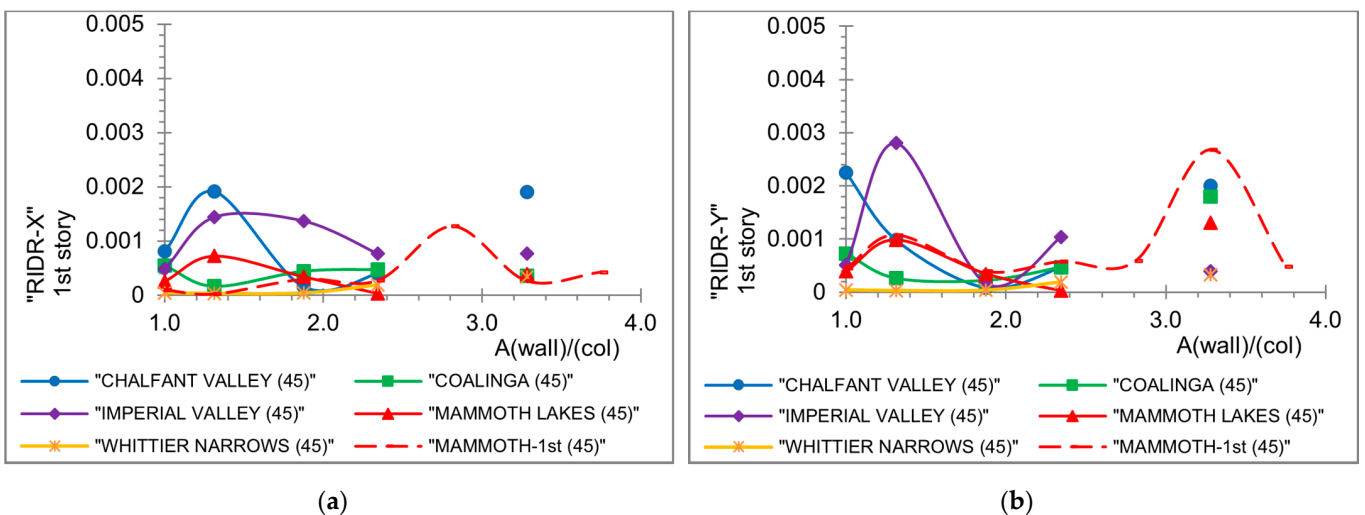
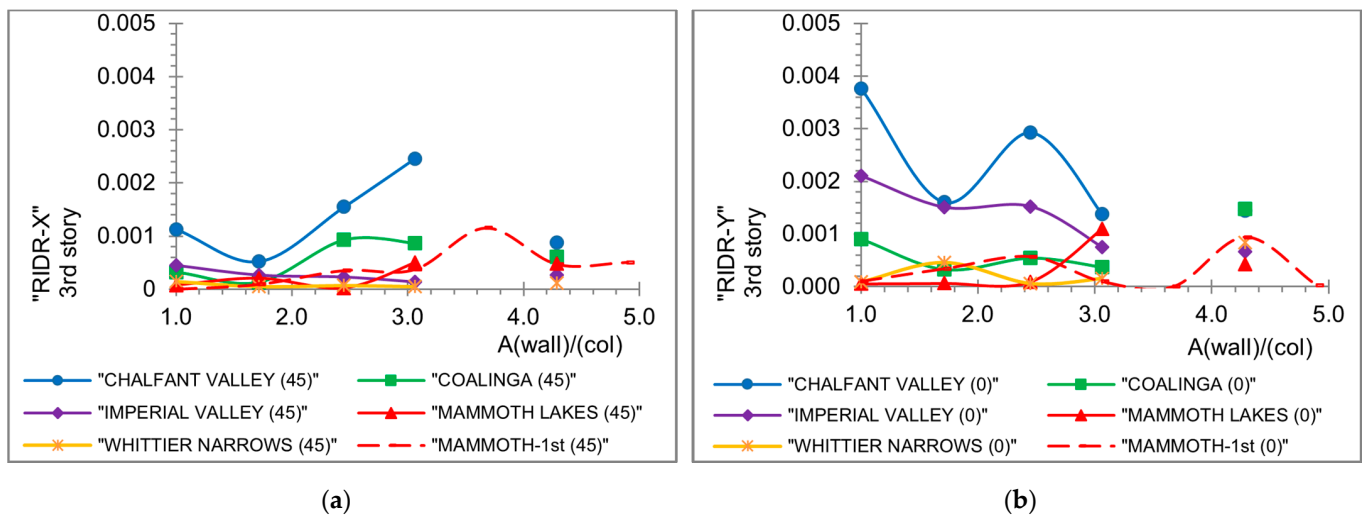


Figure 7. (a) Residual interstory drift ratio on X axis,  $\theta = 45^\circ$ , (b) residual interstory drift ratio on Y axis,  $\theta = 45^\circ$ , 1st story.



**Figure 8.** (a) Residual interstory drift ratio on X axis,  $\theta = 45^\circ$ , (b) residual interstory drift ratio on Y axis,  $\theta = 0^\circ$ , 3rd story.

#### 4. Conclusions

This work investigated the elastoplastic behavior of RC building frames under multiple seismic events and a single seismic one for comparison using NLTH analyses, reaching the following findings.

- (1) The IDR increases with larger wall sections and for higher building frames. In general, the IDR charts tend to have a value range inside the allowed limits of the present seismic regulations.
- (2) The RIDR charts have a general value range inside the allowed constraints of the applicable regulations. The RIDR values for the Y axis are noticed as greater than the corresponding ones for the X axis.
- (3) The direction of the ground excitation influences the seismic response characteristics, while the selected values of  $0^\circ$ ,  $45^\circ$  and  $90^\circ$  are identical for the definition of the most detrimental response values.
- (4) Multiple seismic events tend to deteriorate the strength of RC frames.
- (5) The framed constructions with large wall cross-sections, i.e., greater than the “wall” limit section of present provisions, as well as the symmetrical buildings, are vulnerable to multiple seismic events, in contrast to a single seismic excitation.

**Funding:** This research received no external funding.

**Institutional Review Board Statement:** Not applicable.

**Informed Consent Statement:** Not applicable.

**Data Availability Statement:** Data are contained within this paper.

**Conflicts of Interest:** The author declares no conflict of interest.

#### References

1. Rutenberg, A. *Nonlinear Seismic Analysis and Design of Reinforced Concrete Buildings*, 1st ed.; Fajfar, P., Krawinkler, H., Eds.; Elsevier Science Publishers Ltd.: Essex, UK, 1992; pp. 328–355.
2. Goel, R.K.; Chopra, A.K. Effects of plan asymmetry in inelastic seismic response of one-story systems. *J. Struct. Eng.* **1991**, *117*, 1492–1513. [[CrossRef](#)]
3. Bento, R.; De Stefano, M.; Köber, D.; Zembaty, Z. *Seismic Behaviour and Design of Irregular and Complex Civil Structures IV*, 1st ed.; Springer Nature: Cham, Switzerland, 2022.
4. *Eurocode 2 (EC2); Design of Concrete Structures-Part 1-1: General Rules and Rules for Buildings*. European Committee for Standardization (CEN): Brussels, Belgium, 2004.

5. *Eurocode 8 (EC8)*; Design of Structures for Earthquake Resistance—Part 1: General Rules, Seismic Actions and Rules for Buildings, Part 3: Strengthening and Repair of Buildings, Part 5: Foundations, Retaining Structures and Geotechnical Aspects. Part 6: Towers, Masts and Chimneys. European Committee for Standardization: Brussels, Belgium, 2004.
6. Hatzigeorgiou, G.D.; Beskos, D.E. Inelastic displacement ratios for SDOF structures subjected to repeated earthquakes. *Eng. Struct.* **2009**, *31*, 2744–2755. [[CrossRef](#)]
7. Hatzigeorgiou, G.D.; Liolios, A.A. Nonlinear behaviour of RC frames under repeated strong ground motions. *Soil Dyn. Earthq. Eng.* **2010**, *30*, 1010–1025. [[CrossRef](#)]
8. Lazaridis, P.C.; Kavvadias, I.E.; Demertzis, K.; Iliadis, L.; Vasiliadis, L.K. Structural Damage Prediction of a Reinforced Concrete Frame under Single and Multiple Seismic Events Using Machine Learning Algorithms. *Appl. Sci.* **2022**, *12*, 3845. [[CrossRef](#)]
9. *Eurocode 1 (EC1)*; Actions on Structures-Part 1-1: General Actions, Densities, Self-Weight, Imposed Loads for Buildings. European Committee for Standardization (CEN): Brussels, Belgium, 2001.
10. Askouni, P.K. The Effect of Sequential Excitations on Asymmetrical Reinforced Concrete Low-Rise Framed Structures. *Symmetry* **2023**, *15*, 968. [[CrossRef](#)]
11. ETABS. *Integrated Building Design Software*; Computers and Structures Inc. CSI.: Berkeley, CA, USA, 2015.
12. Pacific Earthquake Engineering Research Center (PEER): Strong Motion Database. Available online: <https://ngawest2.berkeley.edu/> (accessed on 10 September 2022).
13. Rigato, A.B.; Medina, R.A. Influence of angle of incidence on seismic demands for inelastic single-storey structures subjected to bi-directional ground motions. *Eng. Struct.* **2007**, *29*, 2593–2601. [[CrossRef](#)]
14. Sfakianakis, M.G.; Fardis, M.N. Nonlinear finite element for modeling reinforced concrete columns in three-dimensional dynamic analysis. *Comput. Struct.* **1991**, *40*, 1405–1419. [[CrossRef](#)]
15. Sfakianakis, M.G. Computation of Yield and Failure Surfaces for Biaxial Bending with Axial Force of Reinforced Concrete Sections with Jackets. In Proceedings of the 15 WCEE2012, Lisbon, Portugal, 24–28 September 2012.
16. *FEMA-356*; Prestandard and Commentary for the Seismic Rehabilitation of Buildings. Federal Emergency Management Agency: Washington, DC, USA, 2000. Available online: <https://www.nehrp.gov/pdf/fema356.pdf> (accessed on 10 September 2020).

**Disclaimer/Publisher’s Note:** The statements, opinions and data contained in all publications are solely those of the individual author(s) and contributor(s) and not of MDPI and/or the editor(s). MDPI and/or the editor(s) disclaim responsibility for any injury to people or property resulting from any ideas, methods, instructions or products referred to in the content.